sciendo

DOI: 10.2478/ata-2022-0007

Acta Technologica Agriculturae 1
Nitra, Slovaca Universitas Agriculturae Nitriae, 2022, pp. 40–46

CHARACTERISTICS OF DISTANCE ERRORS OF INFRARED SENSOR RELATION TO COLOUR SURFACES

Dušan HRUBÝ, Lukáš VACHO*, Ľubomír KUBÍK, Ladislav TÓTH, Juraj BALÁŽI, Patrik KÓSA, Marián KIŠEV

Slovak University of Agriculture in Nitra, Slovakia

This paper deals with the determination of the absolute errors of a small time of flight (ToF) distance sensor with respect to coloured surfaces at different illumination intensities. The aim was to determine the absolute error of the measured distance by the VL53L1X sensor when set to short-mode and long-mode at different illumination intensities: 10 lx and 350 lx depending on the coloured surface using regression analysis methods. The research was performed using 7 colour samples with different spectral colours determined according to the CIE Lab colour model. Based on the performed experiments, it was found that the error at different sensor settings, change of colour surface and different illumination intensity is approximated by a linear function only up to a certain measured distance. The process is influenced by proposed factors such as: illumination intensity, coloured surface with different illumination reflectance and signal-noise parameters of the tested sensor during the experiment.

Keywords: time of flight distance sensor; distance measurement; colour surface; absolute error; regression analysis

Measuring distances to objects provides important information about environment, especially in areas where obstacles need to be identified around a moving mobile device. Depth or distance sensing play an important role in preventing collisions (Klimenda et al., 2021; Ghandour et al., 2016; Beloev et al., 2021), where different sensors working on different principles can be used. Many types of sensors designed to measure displacement, distance and position in typical applications are based on the time of flight (ToF) principle (Majchrzak et al., 2009; Jans et al., 2020; Chiabrando et al., 2009) with ToF variation implementation. The first principle is based on direct measurement of the runtime of a travelled light pulse; other principle uses amplitude modulated signal for obtaining the distance information by measuring the phase difference between a reference and reflected signal. Miniaturization of optical ToF sensors using electro-optical elements like single-photon avalanche photodiodes (SPADs) or vertical cavity surface-emitting lasers (VCSELs) currently brings new application possibilities (Dutton et al., 2019; Kim and Choi, 2019). In case of IR ToF sensors, the solution offers advantages in the form of angular resolution with the possibility of programming the region of interest (ROI), lower physical form factor and higher frame rates compared to conventional ultrasonic sensors, the use of which can be distorted mainly by environmental factors such as humidity and pressure (Arriaga et al., 2017). Despite the technological advantages of IR ToF sensors (Foix et al., 2011), when used in applications, there are factors such as surface reflectivity that affects the sensor, which can lead to losses in the rate of return of the reflected signal from the object (Jans et al., 2020). This important factor introduces uncertainty into the process of electro-optical non-contact distance measurement, which can affect various applications using a given measurement principle (Zámečníková et al., 2014). The given influences can be analysed and described by regression analysis methods (Bilčík et al., 2019), obtaining thus the necessary information for the subsequent correction of the measured distance (Okubo et al., 2009; Badura et al., 2019). Systematic errors of ToF are typically fixed and their effect can be compensated by calibration under normal circumstances. On the contrary, an unsystematic error is caused by the external environment, and its form is not fixed, which makes it more difficult to create a model to describe and correct this type of error (Foix et al., 2011; He et al., 2017). There are currently several types of inexpensive IR ToF distance sensors that are suitable for a variety of applications (Jans et al., 2020). This paper is focused on the characterization of systematic errors of the IR ToF sensor VL53L1X designed for distance measurement in order to describe the coloured surface influence of a planar object on the measured perpendicular distance by the sensor. Handheld professional laser distance meter was used for the purposes of control and reference distance measurement with which the results are compared. In this work, there is presented a way to describe the distance sensor errors using statistical methods as regression analysis and machine learning-support vector machine, in which the results of methods are reciprocally compared to demonstrate the application suitability to the measured data.

Contact address: Lukáš Vacho, Slovak University of Agriculture in Nitra, Tr. Andreja Hlinku 2, 949 76 Nitra, Slovakia, email: lukas.vacho@uniag.sk

Material and methods

The 8-bit ATmega 2560 microcontroller is used as a communication interface between the sensor and PC. The VL53L1X distance sensor has an I2C communication interface. With this interface, the control of sensor and data collection in connection with the microcontroller is secured. A serial interface with a set communication speed of 115200 baud is used to transfer data from the measuring device to PC. The VL53L1X distance range sensor belongs to the category of miniature ToF electro-optical devices used to emit laser radiation to the environment with a wavelength of 940 nm in laser class 1. SPAD photodiode is implemented in the sensor to receive reflected light beam. Detailed parameters included in technical data of sensor given by the manufacturer (STMicroelectronics, 2018), and selected key parameters are: maximum possible measurable distance – 4000 mm; maximum ranging error – ±25 mm; typical field of view (FoV) – 27°. The VL53L1X distance sensor is designed in a manner that it is possible to measure the distance in several types of modes: short and long. Each measurement includes a set time frame during which the measurement is performed, and the data is sent to the communication bus. This time frame can be set between 20 ms and 1000 ms. In this experiment, value of 30 ms is selected, which is sufficient for data obtaining. Based on the technical data, the minimum possible measurable distance with the sensor is 40 mm, while it is possible to measure a distance of up to 2000 mm in short mode, and up to 4000 mm in long mode under suitable lighting conditions that are not precisely specified quantitatively. For the experiments, repeated measurements are conducted at the level of average value of illumination intensity 350 lx and the average value of illumination intensity 10 lx, which are measured using a professional handheld luxmeter UT383S UNI-T, with a maximum measurement deviation of ±5% and a measurement range from 0 to 199000 lx. The illumination intensity measurement is performed by mechanical connection of the luxmeter with the device on a tripod. The values of illumination intensity at the laboratory are continuously controlled and corrected during the experiment by means of regulated external lighting equipped with an Osram HQI-TS 150 W/NDL halide lamp. Experimental measurements are performed under laboratory standard conditions, with facts on reducing the influence of external lighting on the experimental process. Seven types of plain colour surfaces are used for testing of distances. These surfaces are located in the plane ρT, like described in Fig. 1. The colour spectrum of the given surfaces is determined using a professional spectrophotometer YS3020 3nh by setup CIE Lab colour model. The following tested coloured surfaces with Lab values are used: black (28.92; 0.75; -1.03), blue (43.13; 7.9; -38.72), brown (41.04; 13.22; 12.6), green (63.43; -42.51; 32.10), red (46.63; 48.84; 23.96), white (92.82; 0.84; -6.74), and yellow (82.97; 7.92; 73.16). In experimental measurements, the handheld professional laser distance meter LM50 UNI-T with a measuring accuracy of ±2 mm is used to verify the measured distance accuracy. The device is mechanically connected to the controlled sensor part. The established testing device containing the VL53L1X sensor, microcontroller, and handheld laser distance meter are mounted on a three-point tripod. Principle of the method of measuring distances to coloured planar objects is illustrated in Fig. 1.

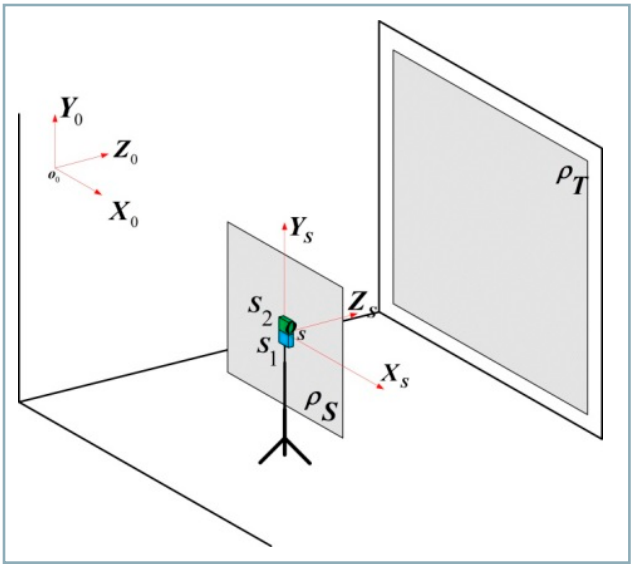


Fig. 1 Representation of distance measurement by a laser ToF sensor

Experimental distance measurement can be characterized by the following coordinate systems:

$$O_0 = (X_0, Y_0, Z_0); \qquad O_S = (X_s, Y_s, Z_s) \tag{1}$$

where:
O_0 – basic coordinate system space of the experiment; O_S – coordinate system of the measuring device

The experiment uses two planes ρ_S and ρ_T. Relations between the plane ρ_S and distance measuring devices (S_1, S_2), and between the plane ρ_T in the form of a thin planar shape can be characterized as follows:

$$S_1 \wedge S_2 \in \rho_S; \qquad \rho_T \perp Z_S^{\rho S} \tag{2}$$

A change in the distance of measuring system in the plane ρ_S to ρ_T, can be described by transformation matrices, determining the position of measuring system in the coordinate system. The measuring system of the distance sensor with the sensor for control distance measurement can be characterized in matrix form as:

$$S_{12}(x_s, y_s, z_s) = [x_s, y_s, z_s, 1] \in \mathbf{R} \ \text{(mm)} \tag{3}$$

By applying the transformation matrix $\mathbf{T_T}$ to $\mathbf{S_{12}}$, one obtains changed position of the measuring system in the following form:

$$\mathbf{S_{12}}' = \mathbf{S_{12}} \times \mathbf{T_T} \ \text{(mm)} \tag{4}$$

According to Eq. 4, the measuring system position is changed during the experiment, with the x_s (mm), y_s (mm) coordinate values being constant during experiment, and

the x_z (mm) coordinate value varying from 100 mm to 2000 mm or from 100 mm to 4000 mm depending on the selected sensor mode. Distance interval from 100 mm to 4000 mm represents the values of distances at which the error measurements are performed, while values of the distance interval are increased by 100 mm during measurement. The measured data by the distance sensor are characterized by the following vector $\mathbf{D_{DS}}$ (mm):

$$\mathbf{D_{DS}} :\in \mathbf{Z}^{+} = \left[C_{N_i}, d_{DS_i}, Sr_{DS_i}, Ar_{DS_i} \right]; \quad i \in \mathbf{Z}\{1...,100\} \quad \text{(mm)} \qquad (5)$$

where:
C_N – counter data set; d_{DS} – set of distance data (mm); Sr_{DS} – set of signal speed data (kilo counts per second – KCPS); Ar_{DS} – set of ambient rates (KCPS)

Each set contains 100 units of measured data, which are obtained at each selected distance to the object. The $\mathbf{D_{DS}}$ data vector is stored in a file on the host computer for further processing. Data for measurement accuracy verification are stored in a vector $\mathbf{d_{RD}}$ (mm), the range of values of which corresponds to the said intervals of 100 mm to 2000 or 100 mm to 4000 mm in steps of 100 mm. The absolute measurement error for each distance can be determined as follows, taking into account the average measured values from d_{DS} (mm) set:

$$\Delta d = \left(\frac{\sum_{i=1}^{j=100} d_{DS}}{j} \right) - d_{RD_m}; \qquad (6)$$

$$m \in \mathbf{Z}\{1..., 20\} \vee m \in \mathbf{Z}\{1..., 40\} \quad \text{(mm)}$$

For resulting values, it is appropriate to use a suitable mathematical expression in the form of an approximation in order to describe the errors, utilizing a linear approximation of absolute error with the following function (Fraden, 2016):

$$\Delta d_{AP} = a + b \cdot M_{VDS}; \qquad M_{VDS} = \left(\frac{\sum_{i=1}^{j=100} d_{DS}}{j} \right) \qquad (7)$$

where:
a and b – regression constants; M_{VDS} – average values of distances (mm)

If data representing a linear model are available, the support vector machine (SVM) method can be used to approximate the data. This data is used as training data. The linear regression of the absolute error using SVM with weight constant w can be expressed in the following form (Rohani et al., 2019):

$$\Delta d_{SVM} = MIN \sum_{n=1}^{p} \left(d_{RD_n} - w_n \cdot M_{VDS_n} \right)^2; \quad w \in \mathbf{R} \quad \text{(mm)} \qquad (8)$$

Qualitative assessment of regression models is performed using statistical methods (Zhou et al., 2020): mean squared error and root mean square deviation. All measured data during the experiment using VL53L1X are stored and available on web repository (Vacho, 2021).

Results and discussion

The statistical set includes 100 measured values for each measured distance, and it was necessary to determine whether the values in set had been distributed according to the normal distribution. The hypothesis of a normal distribution of values was tested using the Lilliefors test at a significance level of $p = 0.05$. The absolute measurement distance error of the VL53L1X distance sensor was evaluated for short mode, long mode, at a low average illumination intensity – 10 lx, and at a higher average illumination intensity of – 350 lx. The measurement results are shown in the following graphs.

The largest relative error value – 38.06 mm – in the given range of all tested distances and coloured surfaces was shown in the experiment with a black colour. Average values of the relative error of distances are shown in Fig. 2. Considering the SVM method, the data were divided into a training sequence and a test sequence in different ratios to achieve the best regression result. Root-mean-square deviation was used to determine the suitability of individual regression methods.

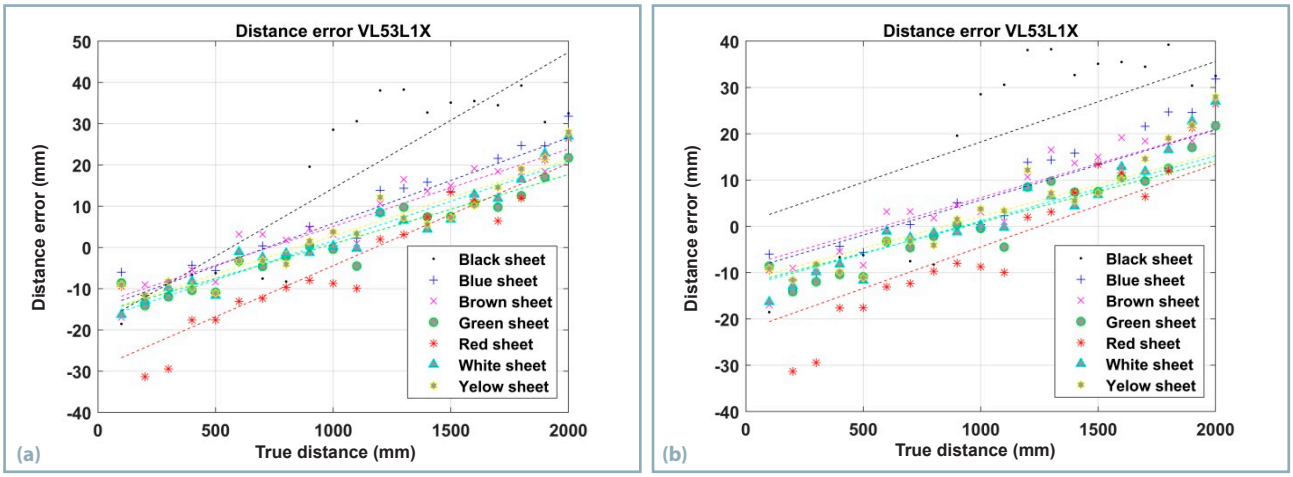


Fig. 2 Representation of the sensor average relative error in short mode at an illumination intensity of 350 lx (a) and representation by using SVM method (b)

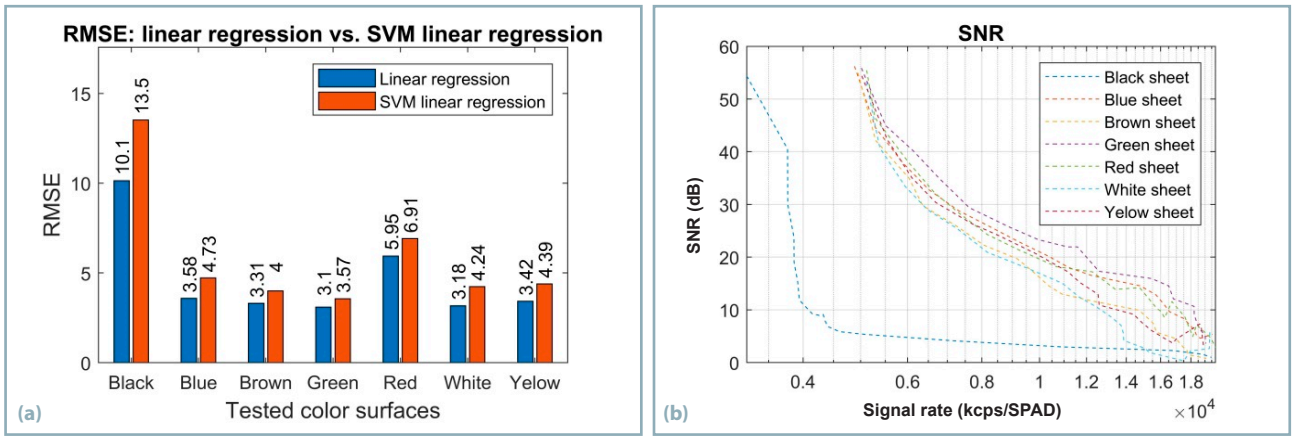


Fig. 3 Comparison of RMSE regression methods for given colours (a) and determination of SNR parameter of individual colours from parameter signal rate at an illumination intensity of 350 lx (b)

The highest value of RMSE was achieved with the black surface and this effect is thus related to the scatter of measured distance values in the statistical set of data for black colour. Furthermore, the results show the equivalence of suitability of regression methods for a sensor mode (short mode), while the SVM shows larger deviations depending on the number of training data sequences. Using the SNR parameter given by the signal-rate to ambient-rate ratio, it was possible to specify the differences in the measured error data, especially in black sheet where it is possible to observe that the value of the SNR ratio decreases significantly with increasing signal rate parameter due to absorption of light emitted by the sensor.

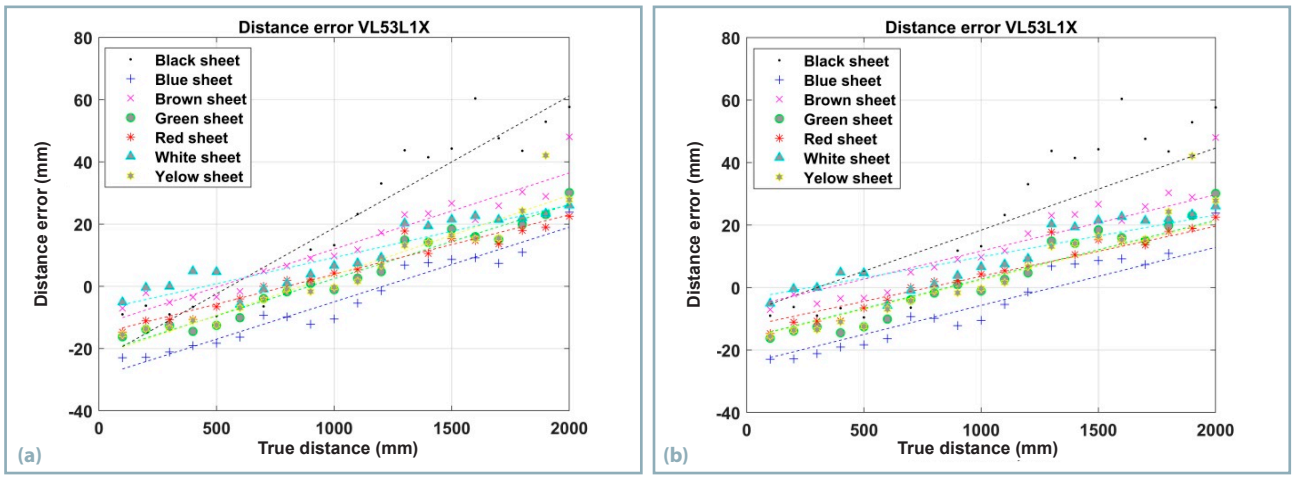


Fig. 4 Relative error of the sensor in short mode at an illumination intensity of 10 lx approximated by linear regression (a) and regression using SVM (b)

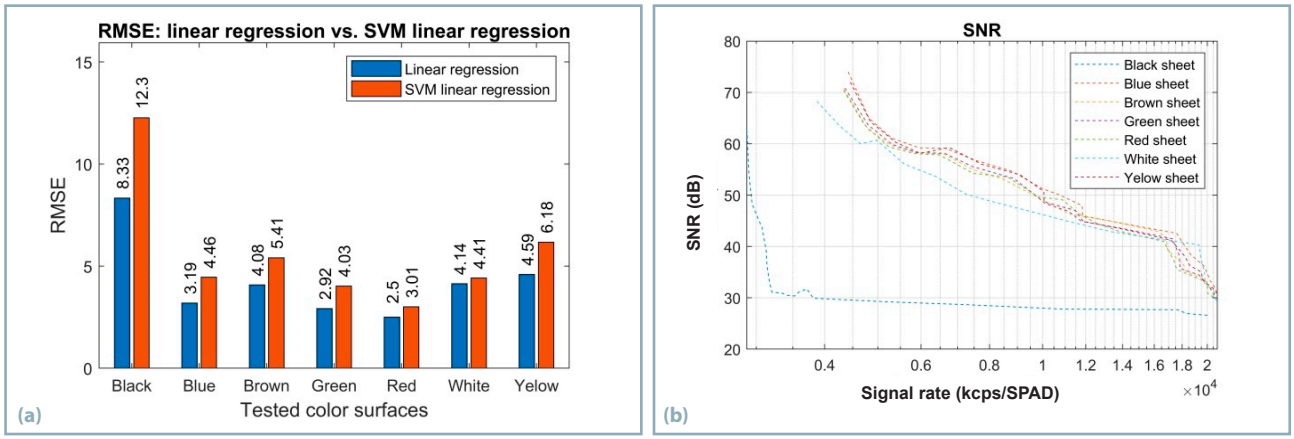


Fig. 5 Comparison of RMSE regression methods for given colours (a) and SNR parameter of individual colours from parameter signal rate at an illumination intensity of 10 lx (b)

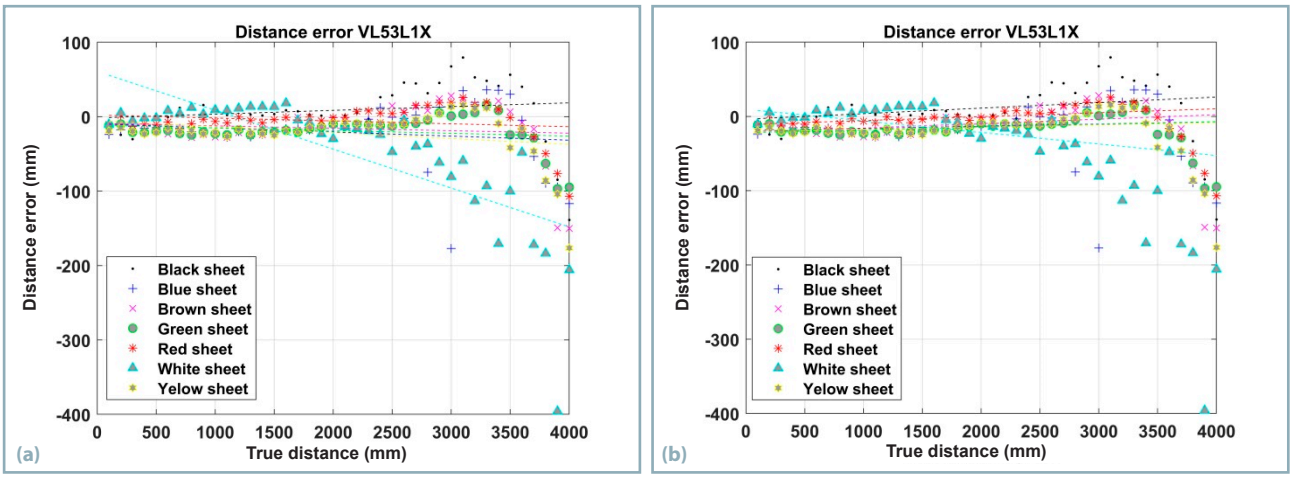


Fig. 6 Relative error of the sensor in long mode at an illumination intensity of 350 lx approximated by linear regression (a) and by regression using SVM (b)

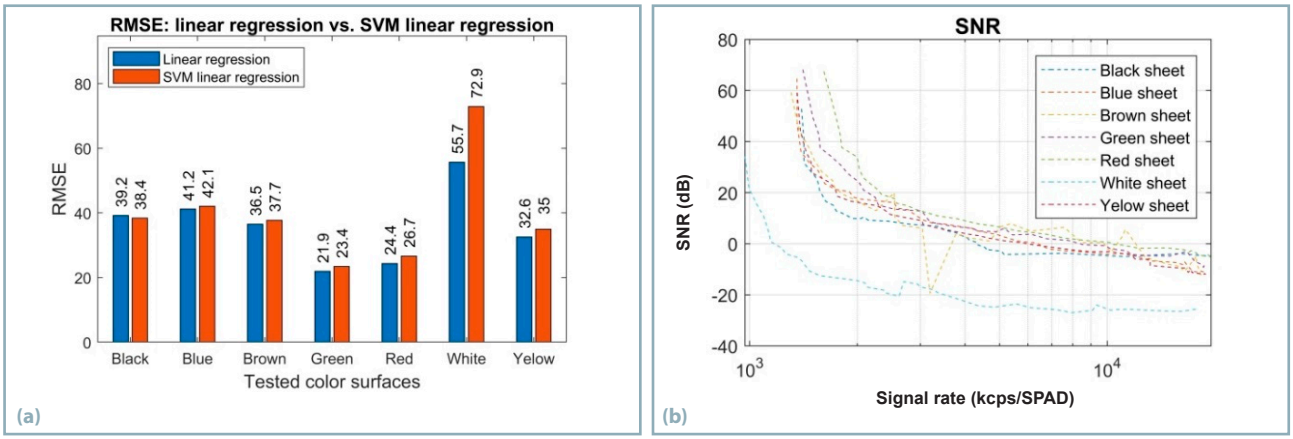


Fig. 7 Comparison of RMSE regression methods for given colours (a) and SNR parameter of individual colours from parameter signal rate at an illumination intensity of 350 lx (b)

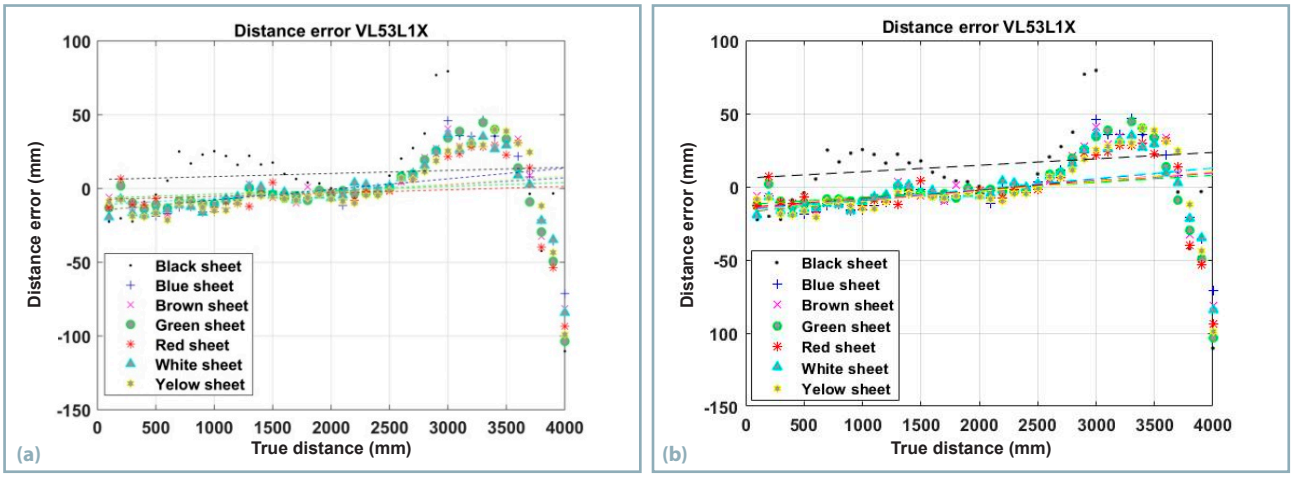


Fig. 8 Relative error of the sensor in long mode at an illumination intensity of 10 lx approximated by linear regression (a) and by regression using SVM (b)

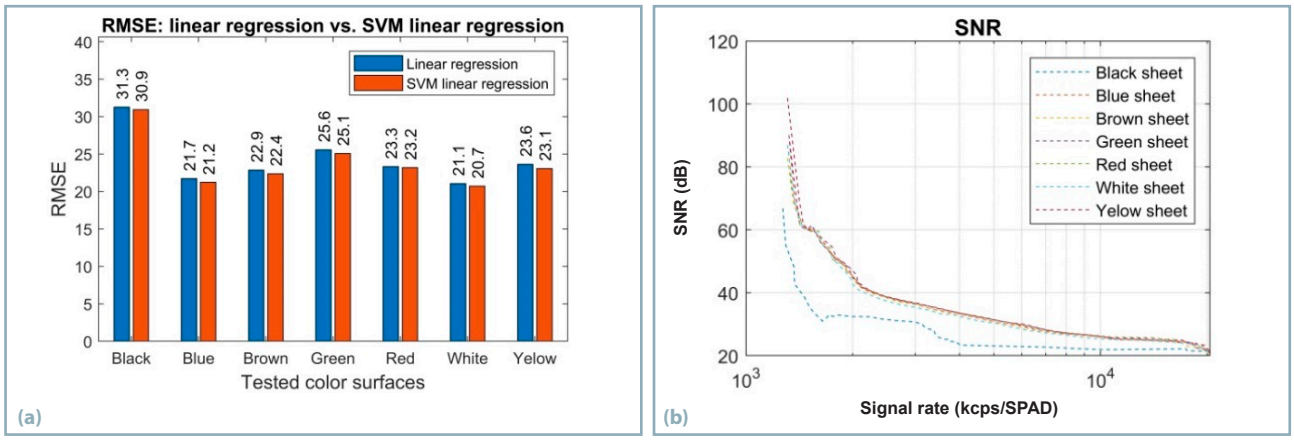


Fig. 9 Comparison of RMSE regression methods for given colours (a) and SNR parameter of individual colours from parameter signal rate at an illumination intensity of 10 lx

Based on the experiment results provided in Figs 4 and 5, it is evident that there are the largest deviations in black even in this case. The average values of relative error of distances at 10 lx illumination intensity are shown in Fig. 4. With reduced illumination intensity in short mode of sensor, there is no significant scattering of distance error values for other colours; therefore, the RMSE values are comparable with the values from the previous experiment with higher illumination intensity. According to the SNR parameter, it is possible to state that the ratio of useful signal is higher in contrast to the previous case due to the increase in the energy radiated by the sensor to achieve the required measured distance.

The average values of relative error of distances in long-mode at 350 lx illumination intensity are shown in Fig. 6. For the purposes of following experiment, only sensors capable of long mode were used – in this mode, it is possible to measure a maximum distance of 4000 m. The experiment results are provided in Figs 6 and 7. In the measurements, a significant variance in the absolute error values at longer distances is noticeable. The difference can also be seen in the RMSE values.

Figures 8 and 9 indicate the experiment results, determining the relative error of the distance sensor at an illumination intensity of 10 lx and in the long mode setting. The average values of relative error of distances in long-mode at an illumination intensity of 10 lx are provided in Fig. 8. Based on the experiment results with a long mode sensor, it is clear that the VL53L1X sensor is nonlinear in a certain area. Such nonlinearity has also been found in other types of ToF sensors that use a light source with an IR spectrum (Chiabrando et al., 2009; He et al., 2017). Nonlinearities cause significant variance in the measured values, limiting thus the sensor applicability in a given setting to its full extent without error compensation. When considering the linear characteristic of IR ToF sensor (Kim et al., 2021) and the occurrence of nonlinearities, it is possible to measure the distance only in a certain (linear) range, otherwise, it is necessary to compensate for errors. Various alternative methods working on different principles can be used to identify and describe the nonlinear dependence of distance error values of sensor (Zhang et al., 2020; Ma and Liu, 2018). When the sensor is set to long mode, the noise level exceeds the useful signal level at 350 lx illuminations in case of black colour. The value of the signal rate did not fall below 10^3 in the case of low and high intensity, ensuring the possibility of distance measuring in distance error interval. Table 1 shows the values of linear regression constants of the absolute measured distance errors by the VL53L1X sensor.

The constants in Table 1 were used in Eq. 7 to determine the linear

Table 1 Constants for linear regression of absolute error determination for used colours

Colour surface	Mode	Constant *a*		Constant *b*	
		350 lx	10 lx	350 lx	10 lx
Black sheet	short	0.032981	0.042394	-18.635842	-23.643526
	long	0.005040	0.002055	-1.581000	6.047192
Blue sheet	short	0.020782	0.023985	-14.929737	-29.006368
	long	-0.005509	0.007179	-9.532423	-14.977654
Brown sheet	short	0.018778	0.024471	-13.698895	-12.523632
	long	-0.003295	0.004545	-8.971115	-11.099385
Green sheet	short	0.016779	0.023857	-15.910789	-21.421947
	long	-0.003690	0.002648	-11.257808	-6.547692
Red sheet	short	0.024804	0.019133	-29.226000	-15.311316
	long	-0.003896	0.002208	2.158308	-7.487577
White sheet	short	0.019095	0.016846	-17.467211	-7.625000
	long	-0.052236	0.004692	60.804538	-11.232731
Yellow sheet	short	0.018593	0.025721	-15.825000	-22.209789
	long	-0.007962	0.005733	-5.375500	-14.347423

dependence of the absolute errors of the distance measured by the VL53L1X sensor.

Conclusion

The aim of presented research was to determine the errors of the IR ToF distance sensor VL53L1X, the use of which is assumed in the applications of reactive navigation of mobile robotics for the detection of obstacles in agriculture and smart agriculture. Determining the properties and errors of ToF distance sensors is important in order to specify the limits of devices that are similar to sensors contained in design. The absolute errors of measuring distances of the VL53L1X sensor used were described by means of regression analysis and regression using SVM, in which the dependence of distance errors on the coloured surfaces was determined. Suitability of the use of regression methods for the IR ToF distance sensor, where a linear characteristic is assumed, was verified by experimental measurements. However, it was found that the sensor also has a non-linear part of characteristics which causes scattering of the measured distance values. Using the described methods, it is possible to test different types of distance sensors that work on the principle of ToF and in the field of IR radiation, as it is possible to determine the limiting factors of sensor use in specific applications with assumed linear character of the absolute error.

Acknowledgements

The research activities in work were supported by project no.: 006SPU-4/2021.

References

ARRIAGA, F. – LLANA, D. F. – ESTEBAN, M. – ÍÑIGUEZ-GONZÁLEZ, G. 2017. Influence of length and sensor positioning on acoustic time-of-flight (ToF) measurement in structural timber. In Holzforschung, vol. 71, no. 9, pp. 713–723.

BADURA, M. – BATOG, P. – DRZENIECKA–OSIADACZ, A. – MODZEL, P. 2019. Regression methods in the calibration of low-cost sensors for ambient particulate matter measurements. In SN Applied Sciences, vol. 1, no. 6, pp. 622.

BELOEV, I. – KINANEVA, D. – GEORGIEV, G. – HRISTOV, G. – ZAHARIEV, P. 2021. Artificial intelligence-driven autonomous robot for precision agriculture. In Acta Technologica Agriculturae, vol. 24, no. 1, pp. 48–54.

BILČÍK, M. – BOŽIKOVÁ, M. – MALÍNEK, M. 2019. The influence of selected external factors on temperature of photovoltaic modules. In Acta Technologica Agriculturae, vol. 22, no. 4, pp. 122–127.

DUTTON, N. A. W. – AL ABBAS, T. – ROCCA, F. M. D. – FINLAYSON, N. – RAE, B. –HENDERSON, R. K. 2019. Chapter 2. Time of flight imaging and sensing for mobile applications. In MAKINWA, K. A. A – BASCHIROTTO, A. – HARPE, P. Low-Power Analog Techniques, Sensors for Mobile Devices, and Energy Efficient Amplifiers. Cham, Berlin : Springer International Publishing, 221–249 pp. ISBN 978-3-319-97870-3.

FOIX, S. – ALENYA, G. – TORRAS, C. 2011. Lock-in time-of-flight (ToF) cameras: A survey. In IEEE Sensors Journal, vol. 11, no. 9, pp. 1917–1926.

FRADEN, J. 2016. Handbook of Modern Sensors: Physics, Designs, and Applications. Berlin : Springer International Publishing, 758 pp. ISBN 978-3-319-19302-1.

GHANDOUR, M. – LIU, H. – STOLL, N. – THUROW, K. 2016. A hybrid collision avoidance system for indoor mobile robots based on human-robot interaction. In Proceedings of the 2016 17^{t} International Conference on Mechatronics – Mechatronika (ME). Prague, Czech Republic: IEEE Explore, pp. 1–7. ISBN 978-80-01-05883-1.

HE, Y. – LIANG, B. – ZOU, Y. – HE, J. – YANG, J. 2017. Depth errors analysis and correction for time-of-flight (ToF) cameras. In Sensors, vol. 17, no. 1, pp. 92.

CHIABRANDO, F. – CHIABRANDO, R. – PIATTI, D. – RINAUDO F. 2009. Sensors for 3D imaging: metric evaluation and calibration of a CCD/CMOS time-of-flight camera. In Sensors, vol. 9, no. 12, pp. 10080–10096.

JANS, R. M. – GREEN, A. S. – KOERNER, L. J. 2020. Characterization of a miniaturized IR depth sensor with a programmable region-of-interest that enables hazard mapping applications. In IEEE Sensors Journal, vol. 20, no. 10, pp. 5213–5220.

KIM, D. – CHOI, J. 2019. Indirect time-of-flight depth sensor with two-step comparison scheme for depth frame difference detection. In Sensors. vol. 19, no. 17, pp. 3674.

KIM, J. – YASUTOMI, K. – KAGAWA, K. – KAWAHITO, S. 2021. High-linearity high-resolution time-of-flight linear-array digital image sensor using time-domain feedback. In Sensors, vol. 21, no. 2, pp. 454.

KLIMENDA, F. – CIZEK, R. – PISARIK, M. – STERBA, J. 2021. Stopping the mobile robotic vehicle at a defined distance from the obstacle by means of an infrared distance sensor. In Sensors, vol. 21, no. 17, pp. 5959.

MA, X. – LIU, Z. 2018. The kernel-based nonlinear multivariate grey model. In Applied Mathematical Modelling, vol. 56, pp. 217–238.

MAJCHRZAK, J. – MICHALSKI, M. – WICZYNSKI, G. 2009. Distance estimation with a long-range ultrasonic sensor system. In IEEE Sensors Journal, vol. 9, no. 7, pp. 767–773.

OKUBO, Y. – YE, C. – BORENSTEIN, J. 2009. Characterization of the Hokuyo URG-04LX laser rangefinder for mobile robot obstacle negotiation. In Unmanned Systems Technology XI., vol. 7332, pp. 279–288.

ROHANI, A. – TAKI, M. – BAHRAMI, G. 2019. Application of artificial intelligence for separation of live and dead rainbow trout fish eggs. In Artificial Intelligence in Agriculture, vol. 1, pp. 27–34.

STMicroelectronics. 2018. VL53L1X Documentation – Description of Distance Sensor VL53L1X.

VACHO, L. 2021. Experimental data – characteristics of distance errors of the small infrared ToF sensor with relation to colour surfaces (experimetal data). Available at: Researchgate: 2021. https://www.researchgate.net/publication/354611120_Characteristics_of_Distance_Errors_of_the_Small_Infrared_ToF_Sensor_with_Relation_to_Colour_Surfaces_Experimental_data

ZÁMEČNÍKOVÁ, M. – WIESER, A. – WOSCHITZ, H. – RESSL, C. 2014. Influence of surface reflectivity on reflectorless electronic distance measurement and terrestrial laser scanning. In Journal of Applied Geodesy, vol. 8, no. 4, pp. 311–326.

ZHANG, M. – ZHOU, J. – SUDDUTH, K. A. – KITCHEN, N. R. 2020. Estimation of maize yield and effects of variable-rate nitrogen application using UAV-based RGB imagery. In Biosystems Engineering, vol. 189, pp. 24–35.

ZHOU, J. – ZHOU, Z. – ZHAO, Q. – HAN, Z. – WANG, P. – XU, J. – DIAN, Y. 2020. Evaluation of different algorithms for estimating the growing stock volume of *Pinus massoniana* plantations using spectral and spatial information from a SPOT6 image. In Forests, vol. 11, no. 5, pp. 540.